Polymorphism of 2,2-Dichloropropane: Crystallographic Characterization of the Ordered and Disordered Phases

P. Negrier,[†] L. C. Pardo,[‡] J. Salud,[‡] J. Ll. Tamarit,*[,‡] M. Barrio,[‡] D. O. López,[‡] A. Würflinger,[§] and D. Mondieig[†]

Centre de Physique Moléculaire, Optique et Hertzienne, UMR 5798 au CNRS-Université Bordeaux I, France, Departament de Física i Enginyeria Nuclear, E.T.S.E.I.B., Universitat Politècnica de Catalunya, Catalonia, Spain, and Institute of Physical Chemistry II, Ruhr-University, Germany

Received January 10, 2001. Revised Manuscript Received December 4, 2001

The polymorphism of 2,2-dichloropropane ($(CH_3)_2CCl_2$) has been further investigated by both thermal and X-ray powder diffraction experiments. From the former the phase transitions between the different phases have been characterized at normal pressure as well as at high pressures (up to 200 MPa). From the $p-T$ slopes of the two-phase coexistence lines, the volume variations at the transition points have been calculated and compared with those obtained by means of X-ray powder diffraction characterization. The existence of two low-temperature stable ordered phases (III and II), one high-temperature orientationally disordered phase (rhombohedral, Ib) and one additional monotropic orientationally disordered phase Ia, has been confirmed. The structure of the low-temperature ordered phase II has been determined by X-ray powder diffraction and Rietveld profile refinement as monoclinic *C*2/*c*, with lattice parameters a =10.6402(3) Å, b = 5.4074(2) Å, c = 10.7295(3) Å, and β = 116.274(3)° at 175.2 K. The strength of intermolecular interactions as well as the anisotropy have been analyzed by means of the thermal-expansion tensor.

1. Introduction

Many organic compounds characterized by globular or pseudospherical molecules exhibit an orientationally disordered high-temperature phase before the liquid state. At low temperatures, the crystal structure of such compounds is characterized by a long-range positional and orientational order. Upon increasing temperature the orientational order is lost first, giving a phase where the molecules are able to reorient on their lattice sites. For this phase the molecules are disposed in a rather symmetrical lattice, generally either cubic or rhombohedral. As the molecules usually display lower symmetry, the compatibility with the higher lattice symmetry is produced by the loss of the orientational order. This orientationally disordered crystalline (ODIC) phase is commonly referred to as the plastic phase.[1,2]

The methylchloromethane compounds, $(CH_3)_{4-n}CCl_n$ (n = 0, ..., 4), belong to this class of materials and are known to display a number of solid−solid-phase transitions.[3−8] Methylchloromethane compounds with n = 2, 3, and 4 are particularly interesting because they are the only ones which display two ODIC phases with two melting points some degrees apart (about 5 K).[3−5,9−14] On cooling from the melt, an ODIC phase (called Ia) is formed, which, upon further cooling, transforms into another ODIC phase Ib. The orientational disorder disappears when the low-temperature ordered phase (phase II) is induced by a first-order phase transition from phase Ib. On warming of the low-temperature ordered phase, phase Ib is formed and remains up to the melting point. However, on heating of phase Ia, it melts without reverting to phase Ib. Thus, phase Ia displays a monotropic behavior that has been extensively studied.[3,4,6,8,9] Earlier birefringence measurements[10,12−14] have unambiguously shown the noncubic symmetry of phase Ib. Actually, X-ray diffraction measurements proved that stable phase Ib is rhombohedral, while metastable phase Ia displays a cubic symmetry.[6]

The polymorphism of 2,2-dichloropropane was studied earlier by Rudman et al.[3,9] The lattice symmetry of stable phase Ib was determined as rhombohedral on the basis of X-ray powder diffraction experiments and from the optical examination of the crystals that revealed the phase as birefringent. This parameter was later ac-

* To whom correspondence should be addressed: Departament de Física i Enginyeria Nuclear, ETSEIB, Universitat Politècnica de Catalunya, Diagonal, 647, 08028 Barcelona, Catalonia, Spain. Tel.: 34 93 401 65 64. Fax: 34 93 401 18 39. E-mail: jose.luis.tamarit@upc.es.
[†] Université Bordeaux I.
[‡] Universitat Politècnica de Catalunya.
[§] Ruhr-University.

(1) Timmermans, J. *J. Chim. Phys.* **1938**, *35*, 331.
(2) Stavely, L. A. K. *Annu. Rev. Phys. Chem.* **1962**, *13*, 351.
(3) Silver, L.; Rudman, R. *J. Phys. Chem.* **1970**, *74*, 3134.
(4) Rudman R. *Mol. Cryst. Liq. Cryst.* **1970**, *6*, 427.
(5) van Miltenburg, J. C. *J. Chem. Thermodyn.* **1972**, *4*, 773.
(6) Pardo, L. C.; Barrio, M.; Tamarit, J. Ll.; López, D. O.; Salud, J.; Negrier, P.; Mondieig, D. *Chem. Phys. Lett.* **2000**, *321*, 438−444.
(7) Tamarit, J. Ll.; López, D. O.; Alcobé, X.; Barrio, M.; Salud, J.; Pardo, L. C. *Chem. Mater.* **2000**, *12*, 555−563.
(8) Pardo, L. C.; Barrio, M.; Tamarit, J. Ll.; López, D. O.; Salud, J.; Negrier, P.; Mondieig, D. *Chem. Phys. Lett.* **1999**, *308*, 204.
(9) Rudman, R.; Post, B. *Mol. Cryst.* **1968**, *5*, 95.
(10) Kogam Y.; Morrison, J. A. *J. Chem. Phys.* **1975**, *62*, 3359.
(11) Anderson, A.; Torrie, B. H.; Tse, W. S. *Chem. Phys. Lett.* **1979**, *61*, 119.
(12) Struts, A. V.; Bezrukov, O. F. *Chem. Phys. Lett.* **1995**, *232*, 181.
(13) Struts, A. V. *Phys. Rev. B* **1995**, *51*, 5673.
(14) Akimov, M. N.; Bezrukov, O. F.; Chikunov, O. V.; Struts, A. V. *J. Chem. Phys.* **1991**, *95*, 22.

10.1021/cm011000g CCC: $22.00
Published on Web 04/03/2002

curately measured from different authors,[14,15] confirming previous observations. In relation to metastable phase Ia, although the patterns were tentatively indexed according to a fcc lattice,[4] a recent work has established without doubt that this phase displays a simple cubic symmetry.[8] The lattice symmetry of the low-temperature ordered phase (II) remained unknown. In addition, Kobashi and Oguni[16] have stated the existence of a new low-temperature ordered phase (hereinafter called phase III), which transforms to phase II at 171.6 K with a very low entropy change (0.06 $kJ \cdot mol^{-1}$). The authors demonstrate the first-order character of the III−II phase transition by the existence of supercooling. In fact, to reach phase III, the sample must be cooled until 80 K. Due to the low entropy change, the transition was associated with slight changes in the positions or orientations of molecules with respect to phase II.

In the present study we report on the polymorphic characteristics of 2,2-dichloropropane and more particularly on the structure of phase II. It will be established that phase II is monoclinic (*C*2/*c*). In addition, we examine the relationship between the orientational molecular disorder and the lattice structures for the different phases of the mentioned compound. It is not our purpose to go further on the thermodynamic properties at normal pressure of 2,2-dichloropropane because the heat capacity has been recently measured in the temperature range between 6 and 300 K [16] and the thermodynamic functions have also been evaluated. Moreover, the authors of that work have analyzed the correlation between thermodynamic properties, especially entropy and volume per molecule, and the molecular sphericity for all the compounds in the series $(CH_3)_{4-n}CCl_n$ ($n = 0$, ..., 4). They have shown that both positional and orientational short-range order of molecules increase with increasing deviation of the molecular shape from spherical. Although the conclusions are well-founded and many details have been analyzed to elucidate such a correlation (absolute entropy was calculated after subtraction of the contribution due to the exchange between positions of the methyl group and chlorine atom within the molecule), the authors based their conclusions on the isomorphism of the orientationally disordered stable phases Ib, which were assumed to be of fcc symmetry. Such a hypothesis is known to be wrong and then the contribution to the entropy change in relation to the translational order of the various compounds of the series should be considered. Fortunately, the overall conclusions are mostly related to the volume occupied by a molecule in the lattice and such a value is found to be very close between the considered fcc lattice and the right value corresponding to the rhombohedral lattice.

2. Experimental Methods

2.1. Material. 2,2-Dichloropropane special grade was supplied by Aldrich Chemical Co. and always handled under an Ar atmosphere without further purification.

2.2. Thermal Analysis at Normal Pressure. Thermal analysis at normal pressure was carried out by means of a Perkin-Elmer DSC-7 instrument equipped with a homemade low-temperature device. Heating and cooling rates of 2 $K \cdot min^{-1}$ and sample masses around 20 mg were used. High-pressure stainless steel pans (also from Perkin-Elmer) were used to prevent sample reactions with the container as well as to resist the high vapor pressure of the compounds.

2.3. Thermal Analysis at High Pressure. The transition temperatures as a function of pressure (up to 200 MPa) were measured in a low-temperature high-pressure apparatus described elsewhere.[17,18] The DTA traces were obtained on heating with scanning rates of about 1 $K \cdot min^{-1}$. The measurements were performed in closed indium capsules containing about 40 mg of the sample. Ar gas was used as a pressure medium. The usual experimental error for the temperature is ±0.5 K. For the pressure measurements the error is ±0.5 MPa.

2.4. X-ray Powder Diffraction. High-resolution X-ray powder profiles were recorded by means of a horizontally mounted INEL cylindrical position-sensitive detector (CPS120)[19] equipped with a liquid-nitrogen INEL CRY950 cryostat (80−460 K) with a temperature accuracy of 1 K and fluctuations lower than 0.3 K. Helium gas was used as a heat exchanger in the sample holder. The detector was used in Debye−Scherrer geometry (transmission mode), enabling a simultaneous recording of the profile over a 2θ range between 4 and 120°. Monochromatic Cu $K\alpha_1$ ($\lambda = 1.54059$ Å) was selected with asymmetric focusing incident-beam curved quartz monochromator.

As recommended,[20] external calibration to convert the measured 4096 channels to 2θ degrees using $Na_2Ca_2Al_2F_4$ cubic phase was applied by means of cubic spline fittings. The peak positions were determined after pseudo-Voigt fitting by using DIFFRACTINEL software.

The liquid samples were sealed in Lindemann capillaries (0.3-mm diameter), which rotated perpendicularly to the X-ray beam during the experiment to improve averaging of the crystallites.

Patterns were obtained at least every 20 K step in the temperature range of the ordered phases (from 90 to 188 K, the temperature of the II−Ib transition) with acquisition times of 120 min. An additional pattern for phase II (at 175.2 K) was measured for structure determination and refinement purposes with an acquisition time of 1115 min. The patterns corresponding to the orientationally disordered stable phase Ib were collected every 5 K between the II−Ib and the melting transitions. As for the orientationally disordered metastable phase Ia, patterns were obtained on cooling at temperature steps close to 3 K from the liquid state to the lowest temperature for which it was possible to metastabilize phase Ia, that is, 184 K. The acquisition times for these measurements were 120 min, a large period of time, which enabled us to improve the peak statistical definition for this high-symmetry lattice.

For all cases the slew rate was 1 $K \cdot min^{-1}$ with a stabilization time of at least 10 min at each temperature before the data acquisition.

3. Results and Discussion

3.1. Thermal Analysis at Normal Pressure. The measured transformation temperatures and entropy changes corresponding to the II−Ib, Ib-L, and Ia-L are given in Table 1. These values are close to previously reported data,[3,5,16] although a noticeable dispersion is found in relation to the melting temperature as a consequence of the differences in the sample purity. Data from ref 16 where the purity was determined to be 99.95% are included in Table 1.

(15) Morrison, A.; Richards, E. L.; Sakon, M. *Mol. Cryst. Liq. Cryst.* **1977**, *43*, 59.
(16) Kobashi, K.; Oguni, M. *J. Phys. Chem. B* **1999**, *103*, 7687.
(17) Würflinger, A. *Ber. Bunsen-Ges. Phys. Chem.* **1975**, *79*, 1195.
(18) Pingel, N.; Poser, U.; Würflinger, A. *J. Chem. Soc. Faraday Trans. 1* **1984**, *80*, 3221.
(19) Ballon, J.; Comparat, V.; Pouxe, J. *Nucl. Instrum. Methods* **1983**, *217*, 213.
(20) Evain, M.; Deniard, P.; Jouanneaux, A.; Brec, R. *J. Appl. Crystallogr.* **1993**, *26*, 563.

Table 1. Temperature Transitions T_c and Entropy Changes ΔS Derived from Calorimetric Measurements at Normal Pressure, Slope of the Temperature−Pressure Two-Phase Equilibria dT_c/dp Derived from Thermal Analysis at High Pressure and Volume Changes Determined from the Clausius−Clapeyron Equation (Δv^{CC}) and from X-ray Powder Diffraction Measurements (Δv^{XR}) for the Different Transitions of $(CH_3)_2CCl_2$[a]

	T_c (K)	T_c* (K)	ΔS* (J·K^{-1}·mol^{-1})	ΔS (J·K^{-1}·mol^{-1})	(dT_c/dp) (K·MPa^{-1})	Δv^{CC} (cm^3·mol^{-1})	Δv^{XR} (cm^3·mol^{-1})
III−II		171.6	0.06				≈0
II−Ib	187.8 ± 0.5	188.2	32.34	32.13 ± 0.62	0.128 ± 0.003	4.1 ± 0.2	4.0 ± 0.7
Ib−L	236.6 ± 0.8	239.6	9.98	9.74 ± 0.45	0.395 ± 0.004	3.9 ± 0.2	5.0 ± 1.0
Ia−L	230.4 ± 1.0			8.38 ± 0.90	0.35 ± 0.12	2.9 ± 0.4	2.3 ± 0.7

[a] Values denoted by (*) are from ref 16.

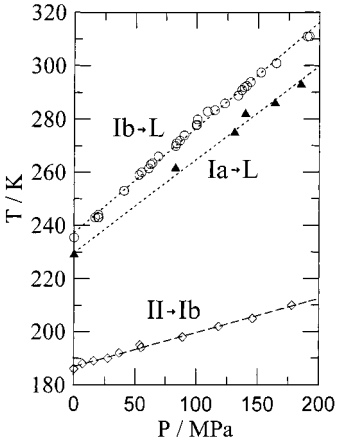

Figure 1. Pressure−temperature phase diagram of $(CH_3)_2CCl_2$. The transition lines have been fitted according to the next polynomials: II−Ib: T(K) = 186.9(0.2) + 0.128(3)·P(MPa); Ib-L: T(K) = 237.3(0.4) + 0.395(4)·P(MPa); Ia-L: T(K) = 229.9-(1.4) + 0.35(12)·P(MPa).

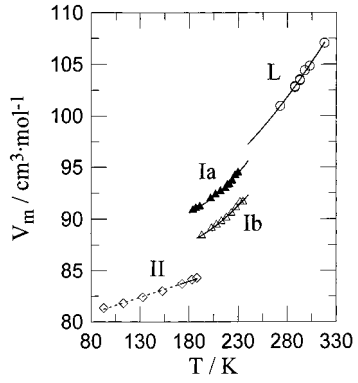

Figure 2. Molar volume of $(CH_3)_2CCl_2$ as a function of temperature derived from X-ray diffraction experiments for the solid phases and from literature for the liquid phase.[23,25]

Although the monotropy of phase Ia was questioned,[15] it has been clearly shown that the required conditions are fully verified: ΔS(Ia-L) < ΔS(Ib-L), ΔH(Ia-L) < ΔH(Ib-L), and T(Ia-L) < T(Ib-L).[21] Assuming that the specific heat of phases Ib and Ia are close and provided that $G_{Ia}(T) - G_{Ib}(T) = [\Delta H_{Ib\rightarrow L} - \Delta H_{Ia\rightarrow L}] - T[\Delta S_{Ib\rightarrow L} - \Delta S_{Ia\rightarrow L}] = 0$, it means that the virtual Ib to Ia transition would take place at a temperature (275.0 K) higher than the melting temperature of both Ia and Ib phases, which shows the monotropy of Ia phase with respect to Ib.

It must be pointed out that the III to II transition temperature reported at 171.6 K has not been detected by thermal analysis because temperatures as low as 80 K cannot be reached with our device.

3.2. Thermal Analysis at High Pressure. The temperature−pressure phase diagram was measured up to 200 MPa (Figure 1). The phase behavior is quite similar to that of CCl_4.[22] That is to say, the monotropic behavior is present for the whole of the analyzed pressure range. It must be noted that the two-phase equilibrium line (Ia-L) has been poorly determined because for many experiments the monotropic phase Ia (metastable) transformed to the stable phase Ib on heating. It can be clearly seen that the slope of the Ib-L equilibrium line is higher than that of the Ia-L line, as was found to be for the same lines in CCl_4. The transition III−II was not detected due possibly to the small associated enthalpy change (around 10 ± 2 J·mol^{-1} according to ref 16) or because the necessary low temperature was not attained.

3.3. Volume Changes. The slopes of the phase transition lines dT_c/dp at normal pressure can be used to calculate the volume changes of the transitions by means of the Clausius−Clapeyron equation. In addition to the slopes, enthalpy changes are needed. Table 1 contains the calculated volume changes. The molar volume changes at the transition temperatures have also been calculated by means of the extrapolated lattice volume at the transformation temperature (see crystallographic characterization or section 3.4). Despite the error of the extrapolated volumes, the values match up satisfactorily.

Figure 2 displays the molar volume for 2,2-dichloropropane as a function of temperature. The molar volumes for liquid phase were obtained from the literature[23−25] while for the solid phases were calculated from the lattice parameters.

3.4. Crystallographic Characterization. a. Phase II. For indexing purposes as well as Rietveld refinement, a pattern for phase II was obtained at 175.2 K with acquisition time of 1115 min. Program DICVOL91[26] was used to determine the lattice symmetry and lattice parameters. By using the first 20 stronger and unambiguously defined reflections, a monoclinic solution came out with lattice parameters of a = 10.641 Å, b = 5.409 Å, c = 10.729 Å, β = 116.3°, and V= 553.7 Å^3 and reliability indices $M(20)$ = 25.3 and $F(20)$ = 21.3. From liquid density data and volume changes (see Table 1),

(21) Grunenberg, A.; Henck, J. O.; Siesler, H. W. *Int. J. Pharm.* **1996**, *129*, 147.
(22) Bardelmeier, U.; Würflinger, A. *Thermochim. Acta* **1989**, *143*, 109.
(23) Timmermans, J.; Delacourt, Y., *J. Chim. Phys. Biol.* **1934**, *31*, 91.
(24) Varushchenko, R. M.; Loseva, O. L.; Skryshevskii, A. F.: Mischenko, N. I.; Matveev, V. K. *Russ. J. Phys. Chem. (Engl. Transl.)* **1987**, *61*, 14; *Zh. Fiz. Khim.* **1987**, *61*, 26.
(25) Clemett, C.; Davies, M. *Trans. Faraday Soc.* **1962**, *58*, 1705.
(26) Louër, D.; Boultif, A. *DICVOL91 Program*; Laboratoire de Cristallochimie, Université de Rennes I: Rennes, France, 1991.

the number of molecules per unit cell was determined to be $Z = 4$. Subsequent refinements were performed using the FULLPROF program as a profile matching tool.[27]

The systematic absences are consistent with the *Cc* or *C*2/*c* space groups (*hkl* reflections with $h + k$ odd and *h*0*l* with *l* odd were absent).[28] The choice of the latter requires 2-fold axes (2 rotation axis and 2_1 screw axis) and normal glide planes (*c* and *n*) and the subsequent refinements seem to verify this as a correct choice. The structure was solved by using the intensities as the starting point in the SHELXL program,[29] which provided a Patterson map. Such a map of vectors between a pair of atoms clearly shows peaks due to "heavy atoms". Large peaks with 0, 2*Y*, $^1/_2$ and 2*X*, 0, $^1/_2 + 2Z$ agree with the *C*2/*c* space group and allow one to calculate the chlorine atomic coordinates. The central carbon atom is on the 2-fold rotation axis with 0, *y*, 0.25 as coordinates. In the initial stage, standard refinement as a rigid body was done. Due to the symmetry, the half unit of $(CH_3)_2CCl_2$ was built up by means of the reported bond lengths and angles obtained from ab initio calculations:[30] 1.521 Å for C−C and 1.798 Å for the C−Cl bonds and 113.0° for the C−C−C and 108.4° for the Cl−C−Cl angles. The methyl group was constructed from SHELXL data as 0.98 Å for the C−H bond and 109.5° for C−C−H and H−C−H angles. The full atomic coordinates were used as the starting point for a Rietveld refinement with the FULLPROF program in the range 18−87° 2θ. The background was linearly interpolated between manually selected experimental points. Final refinement was performed by removing the rigid body constraints for the chlorine and central carbon atoms. The last carbon atom of the asymmetric unit was refined with the hydrogen atoms as a rigid body. The center of such a methyl group was taken on the carbon atomic coordinates and also refined.

The additional refined parameters in the procedure were as follows: the overall scale factor, the lattice parameters, the overall temperature factor, the peak shape parameters (*U*,*V*,*W*), the preferred orientation, the η pseudo-Voigt function (η_0, *X*), and the asymmetric parameters (see Table 2). The Rietveld refinement resulted in an R_B value of 9.5%, R_p of 7.0%, and R_{wp} value of 9.6%. These values confirm the *C*2/*c* space group (No. 15).[28] The collected and calculated profiles are shown in Figure 3 together with the difference plot between them (range cutoff is due to the absence of diffraction lines at lower angles and poor signal at higher angles). The fractional atomic coordinates are collected in Table 3 at 175.2 K. Figure 4 shows the projection of the structure on the *(*00*l*) and the *(h*00) crystallographic planes for $(CH_3)_2CCl_2$. As can be inferred from the results, the structure is ordered, the 2-fold axis of the molecule being coincident with the 2-fold rotation axis of the lattice. This order from a crystallographic point of view is compatible with a dynamic orientational disorder around such a 2-fold axis.

Table 2. Profile Refinement Parameters of Phase II of $(CH_3)_2CCl_2$ at 175.2 K[a]

parameter	value
overall scale factor	0.098(2)
lattice parameters	
a (Å)	10.6402(3)
b (Å)	5.4074(2)
c (Å)	10.7295(3)
β (deg)	116.274(3)
space group	*C*2/*c*
pseudo-Voigt function η_0, *X*	0.49(5), −0.006(2)
asymmetry parameters to 20°	0.103(6))
	0.019(3)
peak shape parameters (*U*,*V*,*W*) (Å)	0.12(1), −0.076(7), 0.023(1)
preferred orientation along *b*	0.047(8)
overall isotropic temperature factor (Å^2)	0.7(1)
R_p	7.0
R_B	9.5
R_{wp}	9.6

[a] Pseudo-Voigt function: $\eta = \eta_o + X \times 2\theta$.

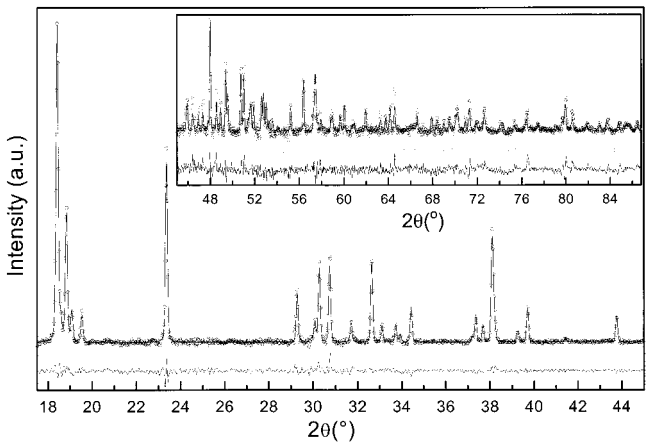

Figure 3. Experimental (○) and theoretical (−) diffraction patterns of phase II for $(CH_3)_2CCl_2$ at $T = 175.2$ K along with the difference profile. Inset corresponds to a ten-times expanded vertical scale for the data from $2\theta \geq 45°$.

Table 3. Fractional Atomic Coordinates for Phase II of $(CH_3)_2CCl_2$ at 175.2 K

atom	*x*	*y*	*z*
C_1	0	−0.1463 (31)	0.25
Cl_1	0.1435 (4)	0.0495 (6)	0.2676 (4)
C_2	−0.0461 (10)	−0.3096 (15)	0.1175 (10)
H_{11}	−0.0746	−0.2028	0.0357
H_{12}	−0.1252	−0.4143	0.1076
H_{13}	0.0324	−0.4143	0.1256

As far as the molecular structure is concerned, the bond lengths and angles obtained after refinement are collected in Table 4. The C−Cl bond has been reported in compounds similar to CH_3Cl (1.778 Å)[31] and to the homologous compounds $(CH_3)CCl_3$ (1.775 Å)[32] and $(CH_3)_3$-CCl (1.81 Å).[7,33] The C−C distance compares also favorably with the accepted values and with those of similar molecules (1.548 Å for $(CH_3)CCl_3$[32] and between 1.53 and 1.57 Å for $(CH_3)_3CCl$[7,33]). With regard to the

(27) Rodriguez-Carjaval, J. *FULLPROF, a program for Rietveld refinement and pattern matching analyses: Abstracts of the satellite meeting on powder diffraction of the XVth congress of the International Union of Crystallography*, Toulouse, France, 1990.

(28) Wilson, A. J. C. *Ed. International Tables for Crystallography, Volume C*; Kluwer Academic Publishers: Dordrecht, The Netherlands, 1992.

(29) Sheldrick, G. M. *SHELXL97, Program for crystal structure refinement*; University of Göttingen: Germany, 1997.

(30) Rey, R.; Pardo, L. C.; Llanta, E.; Ando, K.; López, D. O.; Tamarit, J. Ll.; Barrio, M. *J. Chem. Phys.* **2000**, *112* (17), 7505.

(31) Duncan, J. L. *J. Mol. Struct.* **1970**, *6*, 447.

(32) Silver, L.; Rudman, R. *J. Chem. Phys.* **1972**, *57*, 210.

(33) Rudman, R. *J. Mol. Struct.* **1999**, *485*−*486*, 281.

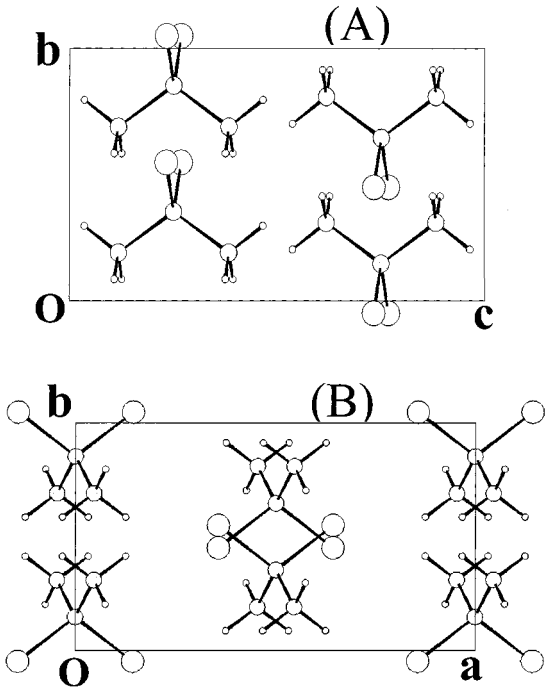

Figure 4. Projections of the monoclinic structure of phase II of $(CH_3)_2CCl_2$ on the (*h*00) (A) and (00*l*) (B) crystallographic plane.

Table 4. Distances and Angles for Phase II of $(CH_3)_2CCl_2$ at 175.2 K

distances (Å)	C−C	1.557
	C−Cl	1.798
	C−H	0.98
angles (deg)	C−C−C[a]	110.9
	Cl−C−Cl[a]	107.8
	C−C−Cl	109.2
	C−C−Cl[a]	109.9
	C−C−H	109.5
	H−C−H	109.5

[a] Calculation made with the symmetry operation $-x, y, {}^1/_2 - z$.

angles involving the central carbon atom, the C−C−C angle (110.9°) is slightly larger than the average value of the C−C−Cl angles (109.5°) and noticeably larger than the Cl−C−Cl angle (107.8°), although close values were obtained for $(CH_3)CCl_3$ and $(CH_3)_3CCl$ (C−C−C, 109.5° and 111.1°; C−C−Cl, 110.2° and 107.9° ; Cl−C−Cl, 108.8°). Finally, it should be mentioned that the intramolecular Cl−Cl distance (2.906 Å) agrees reasonably well with the accepted nonbonded contact radius (between 1.44 and 1.45 Å) for chlorine atoms bonded to the same atom.

The final atomic coordinates were used to calculate the lattice energy by means of the PCK program.[34] Partial charges were taken from ref 30. Such a calculation provides an energy of −57 kJ·mol^{-1} at 0 K. By the addition of the thermal contribution at $T = 175.2$ K, the sublimation enthalpy is determined to be 58.4 kJ·mol^{-1}. From heat capacity data,[16] which enables one to determine the enthalpy difference between 175.2 and 300 K (25.8 kJ·mol^{-1}) and the vaporization enthalpy (31.9 ± 1.0 [35]or 33.1 ± 1.0[36] kJ·mol^{-1}), the experimental sublimation enthalpy ranges between 57.7 and 58.9 kJ·mol^{-1}, that is, (58.3 ± 1.6) kJ·mol^{-1}, which agrees quite well with the calculated value. It must be pointed out that it was verified that small fluctuations of both orientation and position of the molecule in the lattice provided higher energies, which means that the calculated value corresponds to a potential well minimum.

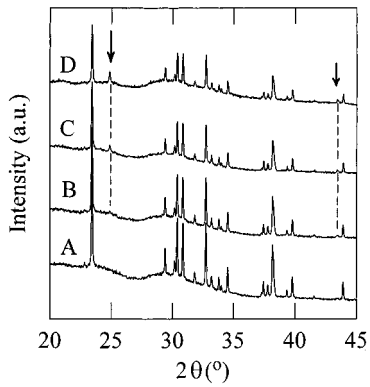

Figure 5. X-ray diffraction patterns corresponding to the transformation from II to III as a function of time at 164.2 K. (A) $t = 0$; (B) $t = 1$ day; (C) $t = 2$ days; (D) $t = 3$ days. Arrows indicate new reflections associated with phase III.

b. Phase III. Following the work of Kobashi and Oguni,[16] phase II was cooled slowly until 80 K and heated again slowly until 164.2 K where an X-ray pattern was obtained. Contrary to what was expected, the pattern was the same as that corresponding to phase II at this temperature. To elucidate the existence of phase III, the sample was maintained at this temperature (i.e., about 10 K below the III−II transition) and X-ray measurements were performed as a function of time for 3 days. Figure 5 shows some of the measured patterns. As can be seen, the pattern obtained after 3 days of maintaining the temperature at 164.2 K is almost identical to that of phase II. Only two new reflections appeared (see arrows in Figure 5), which indicates that, although slowly, a new phase has grown. The intensity of some reflections of phase II diminishes and, after about 40 h, it remains constant. The acquisition was stopped when the intensity of the two new reflections was determined to be constant as a function of time. Soon after, the sample was slowly cooled until 80 K and heated again. Patterns were collected every 10 K until 170 K and from this temperature every 3 K until some degrees above the II−Ib transition temperature. No changes were detected until the III−II transition temperature determined in the previous work.[16] At the transition temperature the new reflections associated with phase III disappear, which corroborates the III−II phase transition.

To characterize the lattice of phase III, the stronger reflections as well as the two new reflections characterizing this phase were used for indexing purposes by means of the DICVOL91 program. It results in a lattice rather similar to that of phase II with a new parameter, b_{III}, close to twice b_{II}, that is, $a = 10.617$ Å, $b = 10.792$ Å, $c = 10.716$ Å, and $\beta = 116.32°$ at 164.2 K. Although this solution indexes all the reflections of the pattern, it is surprising that many other possible reflections do

(34) Williams, D. E. *PCK83 A Crystal Molecular Packing Analysis Program*, Quantum Chemistry Program Exchange 548, University of Louisville, 1983.

(35) Yaws, C. L. *Thermodynamic and Physical Property Data*; Gulf Publishing: Houston, 1992.

(36) Smith, L.; Bjellerup, L.; Krook, S.; Westermark, H. *Acta Chem. Scand.* **1953**, *7*, 65.

Table 5. Polynomial Equations $P = p_o + p_1T + p_2T^2$ (T in K and p in Å or in deg for β Parameter) To Which the Lattice Parameters Were Fitted as a Function of Temperature; R Is the Reliability Factor

phase	temperature range	parameter	p_o	$p_1 \times 10^3$	$p_2 \times 10^5$	$R \times 10^5$
II	93.2−187.5	a	10.476(10)	0.628(15)	0.23(5)	8
		b	5.333(17)	−0.103(24)	0.347(8)	3
		c	10.616(19)	0.674(13)		9
		β	116.42(6)	2.5(8)	−2.2(3)	5
Ib	193.2−235.2	a_H[a]	20.0(7)	0.29(6)	1.2(1.4)	30
		c_H[a]	26.3(1.0)	16(9)	5.8(2.1)	34
Ia	184.2−230.2	a	15.09(36)	−9.5(3)	3.2(8)	32

[a] Polynomials for the lattice parameters of phase Ib correspond to the hexagonal setting of the rhombohedral lattice.

not appear. Because of this experimental fact, it is not possible to find the structure of phase III with some guarantees.

After the performed measurements, one question remains open: Has the transformation from II to III taken place for the whole of the sample? In the work of Kobashi and Oguni,[16] this transformation is supposed to be complete after the sample has been cooled until 80 K. In our experiments, this is not the case and a long period of time aging at a temperature close to but below the III−II transition does not seem to be enough to produce such a transition. The proposed lattice for phase III is physically compatible with the very low entropy change measured for the III−II transition (0.06 $J \cdot K^{-1} \cdot mol^{-1}$).[16] That is to say only slight changes in the orientation of the molecule have occurred. Nevertheless, the possibility that the transformation would have not been completely achieved in the previous work remains an open question. It must be noted that if lattice symmetries of both phases are related by a group−subgroup relationship, it would be quite possible that the difference of the respective heat capacities would be very low. In this line of reasoning it is possible that the dynamic disorder along the 2-fold rotation axis of phase II disappears in phase III, the II to III transition being an ordering transition.

Although dielectric[37] and NMR[14] characterization of phase II for 2,2-dichloropropane were undertaken in the past, there was no indication of the III−II transition.

c. Phase Ib. According to Rudman,[9] the lattice symmetry of stable ODIC phase Ib of 2,2-dichloropropane is rhombohedral with $Z = 21$ and lattice parameters $a = 14.68$ Å and $\alpha \approx 90°$ at 227.2 K; the symmetry results from the optical examination of the crystals which clearly revealed that this phase is birefringent. Morrison et al.[15] reported unambiguous birefringence measurements, confirming the departure from cubic symmetry. Our recent work[6] has confirmed this result and accurate lattice parameters were determined to be $a = 14.730(8)$ Å and $\alpha = 89.41(1)°$ at 232.2 K.

d. Phase Ia. Metastable phase Ia was indexed in the past only tentatively as fcc.[4] Previous thermal measurements could not isolate phase Ia and thus determine the thermodynamic properties associated with the phase transitions.[3] Well-defined X-ray diffraction patterns have been obtained for phase Ia, which could be undercooled (by using a very slow cooling rate) down to 184 K. It is possible that the stability of phase Ia is enhanced by the glass surface of the Lindemann capillary as it was in the birefringence cell.[15]

The patterns were unambiguously indexed by using the DICVOL91 program according to a simple cubic lattice, the parameter being $a = 14.639(5)$ Å at 230.2 K.[6] The pressure−temperature phase diagram enables us to calculate the volume change of the melting of phase Ia and with the liquid density values to calculate Z: this results in $Z = 20$. The melting volume change of phase Ia obtained from the crystallographic data and from the Clausius−Clapeyron equation are in total agreement (see Table 1).

3.5. Thermal Expansion Tensor. To determine the anisotropy of the intermolecular interactions in the solid state, the isobaric thermal expansion tensor has been determined. It is well-known that the deformation of a crystal by a change in the temperature is minimal in the directions of the highest atomic density, that is, the directions of the highest intermolecular interactions. At a given temperature, knowledge of the principal coefficients and of the principal axes directions of the isobaric thermal expansion tensor allows one to determine the directions of the weakest and highest deformation related to the directions of the corresponding intermolecular interactions in the crystal structure. Such directions are commonly referred to as soft and hard directions, respectively.[7,38]

To determine the thermal expansion tensor of $(CH_3)_2CCl_2$, several X-ray patterns were collected for each phase at different temperatures. To enlarge the temperature stability domain of phase II and according to the findings previously described, temperatures as low as 90 K for (metastable) phase II were reached. Such a procedure enables us to dispose of a better determination of the lattice parameter variation with temperature for such a phase. Thus, patterns of phase II were recorded at seven temperatures from 90 K until the II to Ib transition. For enantiotropic phase Ib 9 patterns were obtained between 193 and 235 K. In relation to monotropic phase Ia, 12 patterns have been recorded during the cooling from 230 to 184 K, the lowest temperature where this phase could be metastabilized.

After indexing the patterns, lattice parameters were refined by means of the AFFMAIL program[39] at each temperature. The refined lattice parameters were fitted as a function of the temperature using a standard least-squares method for each parameter. The agreement between the calculated and experimental values has been estimated with the help of the reliability factor, defined as $R = \sum(y_o - y_c)^2/y_c^2$, where y_o and y_c are the measured and calculated lattice parameters, respec-

(37) Turkevich A.; Smyth, C. P. *J. Chem. Phys.* **1940**, *62*, 2468.

(38) Salud, J.; Barrio, M.; López, D. O.; Alcobé, X.; Tamarit, J. Ll. *J. Appl. Crystallogr.* **1998**, *31*, 748.

(39) Rodríguez-Carvajal, J. *AFMAIL* program; Laboratoire Leon Brillouin, CEA-CNRS: France, 1985.

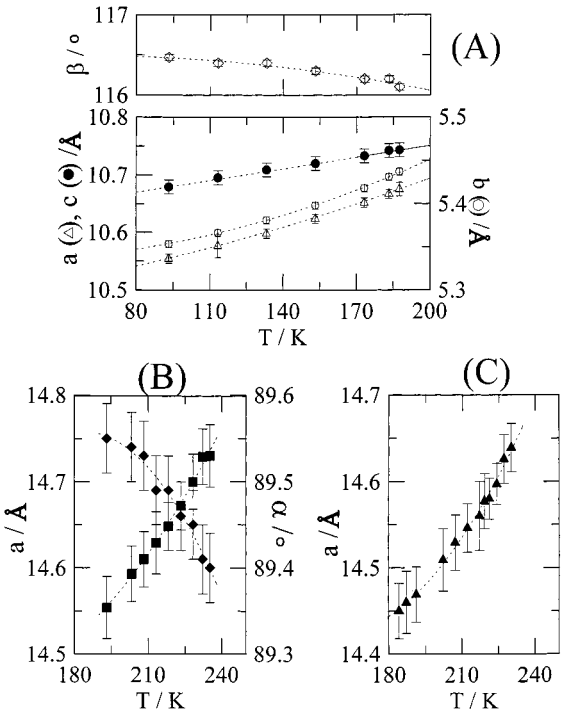

Figure 6. Lattice parameters of $(CH_3)_2CCl_2$ for phases II (A), Ib (B), and Ia (C) as a function of temperature. For T < 171.6 K, values correspond to the undercooled phase II.

tively. Table 5 gathers the coefficients of the polynomial equations. Such polynomial equations are plotted together with the experimentally determined lattice parameters in Figure 6 for the different phases.

The lattice deformation dU due to a small temperature variation dT is expressed by a second-rank tensor (α_{ij}), $du_{ij} = \alpha_{ij}\, dT$, the coefficients of the thermal expansion tensor being expressed in K^{-1}. The procedure and the method to determine the principal coefficients as well as the direction of the principal axes of the tensor have been published elsewhere.[38,40] The program DEFORM [41] was used for the calculation of the tensor.

Phase III and Phase II. The tensor of a monoclinic lattice is completely defined by the principal coefficients (α_i, i = 1, 2, 3) and by an angle between the direction of one of the principal directions (α_3 in this case) and one of the crystallographic axes (**c** in this case), the α_2 axis being coincident with the binary **b** axis of the lattice.

Figure 7 depicts the variation of the principal coefficients of the thermal expansion tensor as a function of temperature. In the whole temperature range of phase II studied the α_3 direction corresponds to the hardest direction, which, as can be seen in Figure 8A (where a three-dimensional plot of the isobaric thermal expansion tensor for this phase is presented), is relatively close to the **c** crystallographic direction. This experimental result indicates that in such a direction strong intermolecular interactions are present. This evidence agrees with the determined structure (see Figure 4) for which molecular dipoles almost parallel to the axis b seems to be placed in two-parallel interacting zigzag (with opposite orientation of the dipole) chains. The other two directions, α_1 and α_2, display relatively low values of the principal coefficients in the low-temperature range studied, although upon increasing temperature, both directions become softer. It must be noticed that despite the short intermolecular distances in the **b** crystallographic direction, the interaction in this direction is found to be weak, possibly due to the special arrangement of the dipoles, which are oriented in a head-to-head order providing a diminution

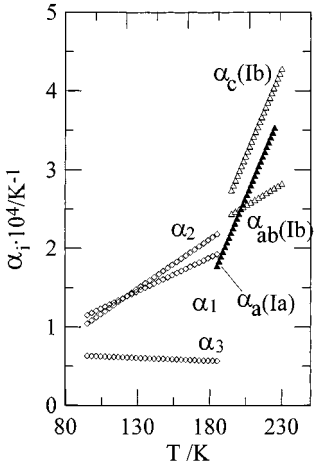

Figure 7. The α_i principal coefficients as a function of temperature for $(CH_3)_2CCl_2$: (◇) phase II (α_2 is chosen parallel to the crystallographic direction **b** in the monoclinic phase), (△) phase Ib, and (▲) phase Ia. For T < 171.6 K, values correspond to the undercooled phase II.

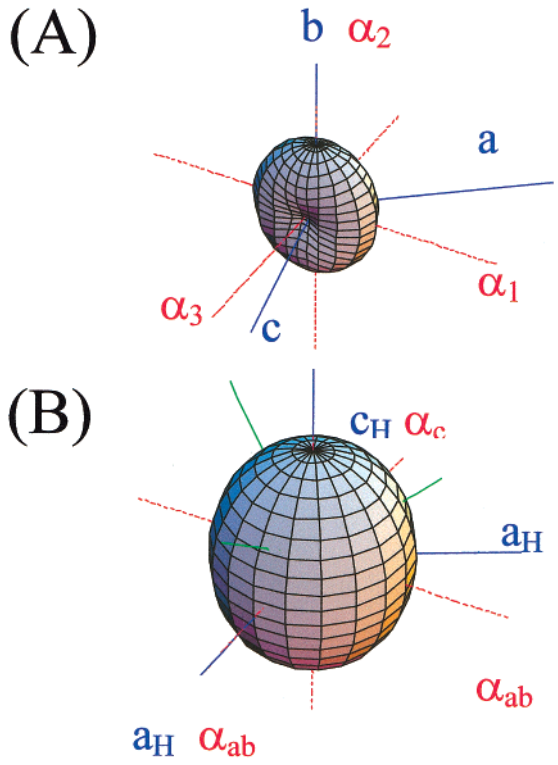

Figure 8. The thermal expansion tensors of phases II at T = 175.2 K (A) and Ib at T = 200.2 K (B) in the frame of the principal directions α_1, α_2, and α_3 (dotted red line) together with the crystallographic axes **a**, **b**, and **c** (continuous blue line) for $(CH_3)_2CCl_2$. In B the axes of the rhombohedral setting (see text) are also shown (green lines). The full length of the α_i axes corresponds to 10^{-3} K^{-1}.

(40) Chanh, N. B.; Clastre, J.; Gaultier, J.; Haget, Y.; Meresse, A.; Lajzerowicz, J.; Filhol, A.; Thomas, M. *J. Appl. Crystallogr.* **1988**, 21, 10.

(41) Filhol, A.; Lajzerowicz, J.; Thomas, M. *DEFORM* program, unpublished software, 1987.

of the intermolecular interaction. Such anisotropy in the principal coefficients means that the intermolecular interactions joining the molecules of 2,2-dichloropropane are highly anisotropic. As we will see later, this anisotropy remains even in the orientationally disordered stable phase Ib.

With respect to the phase III thermal expansion tensor, the results are rather similar to those of phase II, proving that intermolecular interactions would be quite similar in both phases.

Phase Ib. To make evident the anisotropy of the thermal expansion tensor in this orientationally disordered phase, the rhombohedral lattice has been described in terms of a hexagonal lattice ($a_H = 2a_R \sin(\alpha_R/2)$; $c_H = a_R[3(1 + 2\cos\alpha_R)]^{1/2}$; see Table 5). In this description the 3-fold axis **c** must be, according to the Newmann principle (for which the thermal-expansion tensor has to display the point group symmetries of the crystal), a revolution axis of the tensor; that is, the intermolecular interactions in the (00*l*) plane are independent of the direction. In this way the principal coefficients as well as the principal directions can be reduced to two nondependent directions: $\alpha_{\mathbf{c}}$ which is parallel to the **c** crystallographic direction and to $\alpha_{\mathbf{ab}}$ which accounts for the thermal expansion in any direction of the (00*l*) plane. Figure 8B displays the three-dimensional plot of the tensor for this phase. In Figure 7 the values of the principal coefficients are plotted as a function of temperature. As can be seen, the molecular interactions in the $\alpha_{\mathbf{c}}$ direction (which is also the **c** crystallographic direction of the hexagonal description) are softer than those in the (00*l*) plane ($\alpha_{\mathbf{ab}}$). Such anisotropy reinforces the small deviation of the Ib phase from the cubic symmetry.

Phase Ia. Because of the cubic symmetry of this monotropic phase, the tensor is completely isotropic. The value of the principal coefficient (cubic symmetry reduces to only one independent value and the direction of the principal axes are coincident with the crystallographic directions) is determined (see Figure 7) to be between the $\alpha_{\mathbf{c}}$ and the $\alpha_{\mathbf{ab}}$ values of the phase Ib. This result is fully expected because of the small differences between phases Ib and Ia.

Volume Expansivity, Packing Coefficient, and Aspherism Coefficient. The volume expansivity α_V (equal to $\alpha_1 + \alpha_2 + \alpha_3$) is depicted in Figure 9A as a function of temperature for phases II, Ib, and Ia. The lowest volume expansivity corresponds to phase II as a consequence of the higher intermolecular interactions. Concerning the orientationally disordered phases, volume expansivities are quite similar, although in the high-temperature region it seems that phase Ia becomes softer. It must be taken into account that this phase melts 5 K lower than phase Ib and, thus, thermal excitation of phonon vibrational modes must be higher.

Figure 9B shows the variation of the packing coefficient ($\eta = V_m/(V/Z)$, where V_m is the volume of the molecule, 92.17 Å^3, and V/Z is the volume occupied by a molecule in the lattice) for the different phases as a function of temperature. As can be seen, the packing coefficient of phase II, where the highest intermolecular interactions are known to be present, is the highest. Moreover, the packing of phase Ia is, whatever the temperature, lower than that corresponding to phase

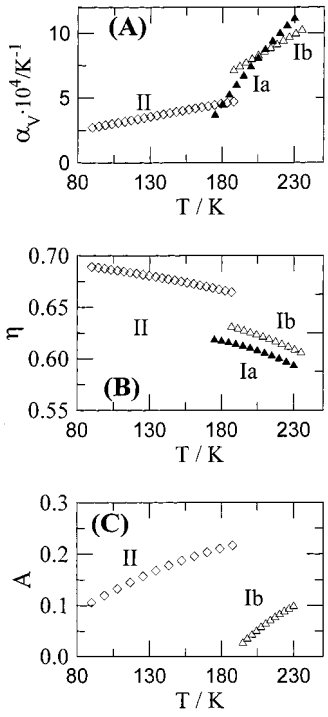

Figure 9. The volume expansivity (α_v) (A), the packing coefficient (η), and the aspherism index (A) as a function of the temperature for phases II, Ib (B) and Ia of $(CH_3)_2CCl_2$ (C). For $T < 171.6$ K, values correspond to the undercooled phase II.

Ib, matching up the stability criterion between both phases; that is, the packing of the monotropic phase (Ia) is smaller than that of the enantiotropic phase (Ib). It must be noticed that the packing value of these orientationally disordered phases is relatively high when compared to other plastic phases for which the existence of dynamical hydrogen bonds has been clearly demonstrated.[34,42] This experimental fact means that some kind of short-range interactions are present in these disordered phases, giving rise to the existence of a short-range order.

The details of the anisotropy of the intermolecular interactions are accounted for by means of the aspherism index, defined as

$$A = (^2/_3)[1 - (3\beta/\alpha_v^2)]^{1/2}$$

where $\beta = \alpha_1\alpha_2 + \alpha_2\alpha_3 + \alpha_1\alpha_3$.[43] The variation of the aspherism index for phases II and Ib with temperature is depicted in Figure 9C. The aspherism index increases with temperature as a consequence of the increasing in the anisotropy of the intermolecular interactions for both phases II and Ib. It should be noted that, for the low-temperature ordered phase II, the aspherism index is of the same order as that of monoclinic low-temperature phase IV of $(CH_3)_3CCl$, where a strong dipole−dipole interaction due to a head-to-tail arrangement of the molecules is present.[7] Concerning the orientationally disordered phase Ib, the aspherism is considerably higher taking into account the disordered character of this phase. This anisotropy is almost of the same order

(42) Tamarit, J. Ll.; Barrio, M.; López, D. O.; Haget, Y. *J. Appl. Crystallogr.* **1997**, *30*, 118.
(43) Weigel, D.; Beguemsi, T.; Garnier, P.; Gerad, J. F. *J. Solid State Chem.* **1978**, *23*, 24.

as that for the librational high-temperature phase of $(CH_3)_3CCN$. This fact points out the existence of weak preferred orientations of molecules, another proof of the uniaxial nature of this phase. It should be noticed that this result was shown in a previous NMR and birefringence study,[14] where the authors analyzed the orientational order parameter in phase Ib.

Finally, it is quite evident that according to the cubic symmetry of phase Ia, the thermal expansion tensor of this phase is isotropic ($A = 0$).

4. Conclusions

The polymorphic behavior of $(CH_3)_2CCl_2$ has been studied from 80 K to the liquid state by means of X-ray powder diffraction measurements.

The structure of the low-temperature ordered phase II has been determined to be monoclinic *C*2/*c* with lattice parameters $a = 10.6401(3)$ Å, $b = 5.4074(2)$ Å, $c = 10.7296(3)$ Å, and $\beta = 116.274(3)°$ at 175.2 K.

The existence of the lowest temperature phase III, previously found throughout heat capacity measurements,[16] has been stated. Nevertheless, the structure of this phase has not been determined because of the very slow growth from phase II. Despite this limitation, it seems to be that phase III is very close, from a structural point of view, to phase II, the difference being on the **b** crystallographic parameter, which doubles.

As far as the orientationally disordered phases are concerned, the enantiotropic−monotropic character of phases Ib−Ia, respectively, has been corroborated. Despite the disorder, the existence of weak preferred orientations of molecules in phase Ib has been demonstrated. Moreover, close similarity between orientationally disordered phases Ib and Ia is found when physical properties, which do not account for the anisotropy properties, as volume expansivity and packing coefficient, are analyzed.

Acknowledgment. This work has been supported by the Spanish DGE under Grants PB98-0923 and PB95-0032. One of us (L.C.P.) would like to acknowledge the fellowship from the Generalitat de Catalunya who enables us to perform the high-pressure measurements at the German laboratory (University of Bochum). The authors are grateful to Prof. J. M. Leger (University of Bordeaux II) for his help in the use of the SHELXL97 program. It is also a pleasure to thank one of the referees for his helpful discussion on the structural part of the manuscript.

Supporting Information Available: Table of lattice parameters corresponding to the phases II, Ib, and Ia of $(CH_3)_2CCl_2$ at some selected temperatures (PDF). This material is available free of charge via the Internet at http://pubs.acs.org.

CM011000G